



Improving landslide susceptibility assessment using satellite data

Dalia Kirschbaum, NASA GSFC, Code 617

The existing global landslide susceptibility map proposed by Hong et al. (2007) (Fig.1) has a coarse spatial resolution ($0.25^\circ \times 0.25^\circ$) and requires improvement in accurately identifying susceptible landslide conditions.

This preliminary research uses an empirical and statistical approach to relate available landslide inventories in the U.S. to slope and relief datasets calculated from the Shuttle Radar Topography Mission (SRTM) database.

The research considers the relationships between maximum slope at 1 km area and relief to establish a threshold which approximately separates susceptible and non-susceptible areas. Work is ongoing to establish an optimum threshold for computing a new susceptibility map.

Relief vs. Slope Max at 10% Cumulative Frequency

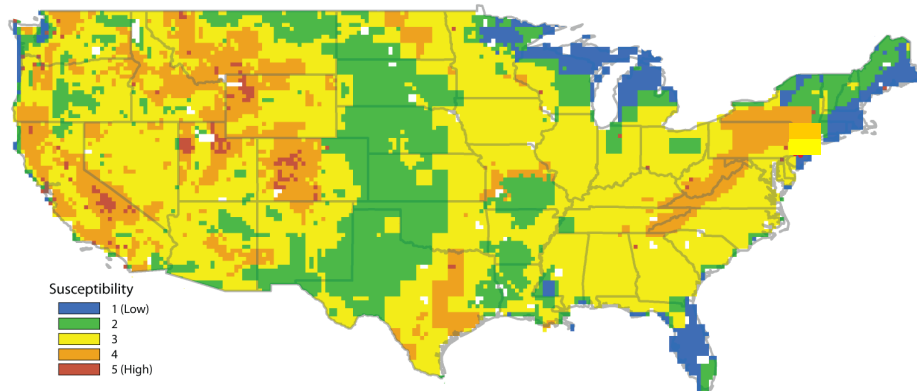
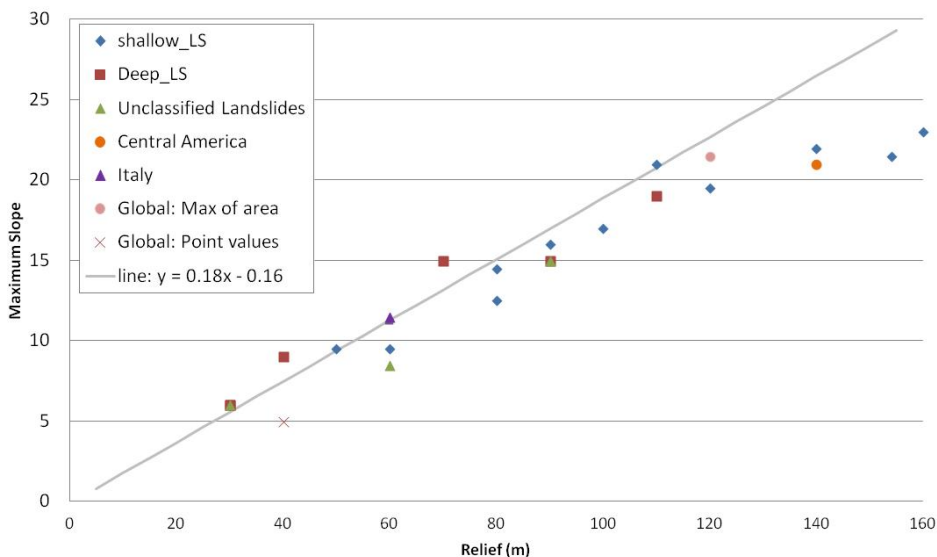


Figure 1: Global landslide susceptibility map from Hong et al. (2007) for the United States

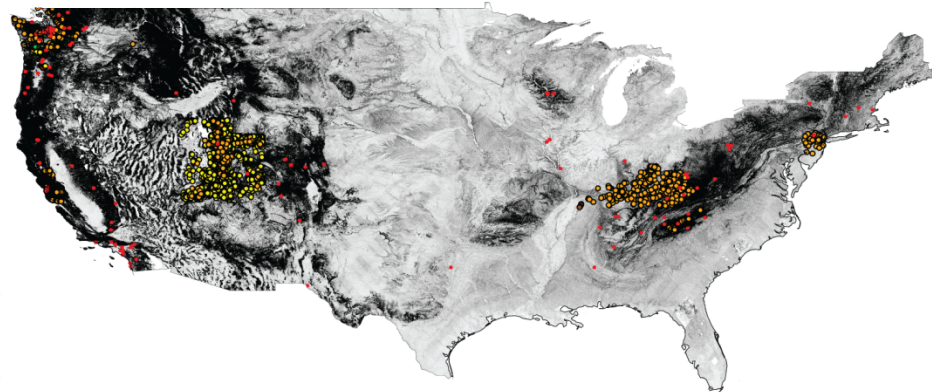


Figure 2: Maximum slope at 1km resolution calculated from the 90m SRTM dataset (Godt et al. 2012) shown with landslide inventories from various states within the U.S. These inventories were used to evaluate the relationship between relief and maximum slope.

Figure 3: Values of the landslide inventory specifying the relief (x-axis) and maximum slope (y-axis) corresponding to the 10% cumulative frequency for each landslide inventory dataset considered. Landslide inventories were divided into shallow, deep and unclassified inventories. Other non-U.S. datasets were also plotted and follow a similar distribution. The grey line indicates the approximate relationship identified by Godt et al. (2012) for the smaller number of case studies considered.



Name: Dalia Kirschbaum, NASA/GSFC, Code 617

E-mail: dalia.b.kirschbaum@nasa.gov

Phone: 301-614-5810

References:

- Hong, Y., Adler, R., & Huffman, G. (2007). Use of satellite remote sensing data in the mapping of global landslide susceptibility. *Natural Hazards*, 43(2), 245-256. doi:10.1007/s11069-006-9104-z
- Godt, J. W., Coe, J. A., Baum, R. L., Highland, L. M., Keaton, J. R., & Roth Jr, R. J. (2012). Prototype landslide hazard map of the conterminous United States. *Symposium A Quarterly Journal In Modern Foreign Literatures*.
- Kirschbaum, D.B., Adler, R., Adler, D., Peters-Lidard, C., and Huffman, G. (accepted). Global Distribution of Extreme Precipitation and High-Impact Landslides in 2010 Relative to Previous Years, *Journal of Hydrometeorology*.
- Kirschbaum, D. B., Adler, R., Hong, Y., & Lerner-Lam, A. (2009). Evaluation of a preliminary satellite-based landslide hazard algorithm using global landslide inventories. *Natural Hazards And Earth System Sciences*, 9, 673-686.

Data Sources: Shuttle Radar Topography Mission (SRTM) digital elevation model, Global Landslide Catalog, several state or regionally-based landslide inventories

Technical Description of Images: The global landslide susceptibility map developed by Hong et al. (2007) provides a global picture of susceptibility from low (1) to high (5) at 0.25°x0.25° resolution. **Fig. 1** shows the susceptibility calculations over the U.S. and highlights the coarse spatial resolution of the existing map, which is currently used within the Global Landslide Forecasting Algorithm and has several limitations described in Kirschbaum et al. (2009). In an attempt to improve the susceptibility map, this preliminary research tests the relationship between relief (calculated as the difference between the maximum and minimum slope of 90m pixels within a 1km grid), maximum slope (calculated as the maximum slope value of 90m pixels within a 1km grid) and available landslide inventories. **Fig. 2** illustrates the maximum slope values from low (white) to high (black) along with available landslide inventories compiled from a variety of different sources, including state and local geological surveys, individual studies, and independent collection. The juxtaposition of these two maps highlights the large resolution differences as well as the possibility of applying a more empirical and statistical approach to calculate susceptibility rather than the statistical/heuristic approach used by Hong et al. 2007. **Fig. 3** provides a scatter plots showing the relief (x-axis) and maximum slope (y-axis) values corresponding to the 10% cumulative frequency distribution for each landslide inventory considered in this analysis. The landslide inventories have been divided by type (shallow/deep) and tend to have a linear relationship when comparing relief and maximum slope values. This approximately corresponds to the linear fit calculated by Godt et al. (2012) when they performed a similar evaluation over the continental U.S.

Scientific Significance: This preliminary investigation tests a different way to calculate susceptibility based solely on two topographic variables, which serves to both decrease errors associated with incorporating multiple datasets from different and variable sources as well as increase the simplicity of the calculations so it is easily transferable to other regions. Future work will consider the optimal threshold by which to relate relief and slope values through considering inventories from other topographically complex regions around the world. This analysis also represents a unique attempt to incorporate as many available landslide inventories as possible in order to evaluate the physical relationship between topography and landslide occurrence and to better estimate landslide susceptibility based on existing data.

Relevance for future science and relationship to Decadal Survey: Precipitation information from TRMM and the upcoming Global Precipitation Measurement (GPM) mission (www.gpm.nasa.gov) will help to relate static landslide susceptibility information ("where" landslides may occur) to precipitation triggers ("when" landslides may be triggered). Soil moisture information, such as from the SMAP mission will also provide important clues to antecedent soil moisture status, allowing us to discern whether a previous rainfall event may play a role in future landslide activity.



Fog- and cloud-induced aerosol modification observed by the Aerosol Robotic Network (AERONET)

Thomas F. Eck, NASA GSFC, Code 618 and Brent N. Holben, NASA GSFC, Code 618

Large fine mode (sub-micron radius) dominated aerosols in size distributions retrieved from AERONET have been observed after fog or low-altitude cloud dissipation events. These column-integrated size distributions have been obtained in many regions of the world, typically after evaporation of low altitude cloud such as stratocumulus or fog. Retrievals with cloud processed aerosol are sometimes bimodal in the accumulation mode with the larger size mode often $\sim 0.4 - 0.5 \mu\text{m}$ radius (volume distribution); the smaller mode typically ~ 0.12 to $\sim 0.20 \mu\text{m}$ may be interstitial aerosol that were not modified by incorporation in droplets and/or aerosol that are less hygroscopic in nature.

Observed trends of increasing aerosol optical depth (AOD) as fine mode radius increased suggests higher AOD in the near cloud environment and therefore greater aerosol direct radiative forcing than typically obtained from remote sensing, due to bias towards sampling at low cloud fraction.

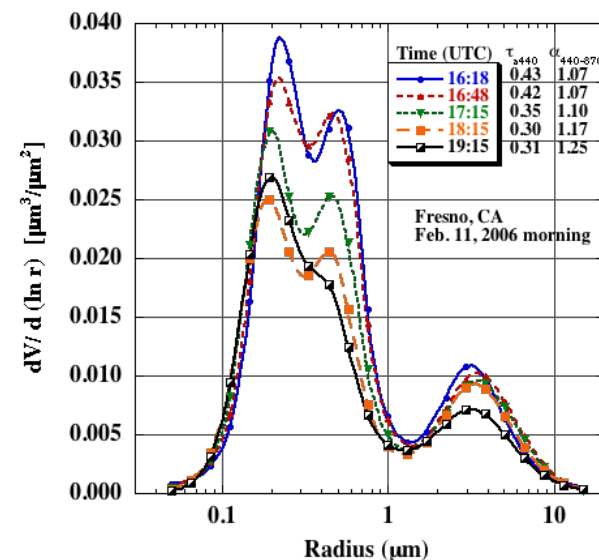


Figure 1: Almucantar size distribution retrievals from Fresno, CA on the morning of 11 February 2006 over a time interval of 3 h for these five almucantar scans.

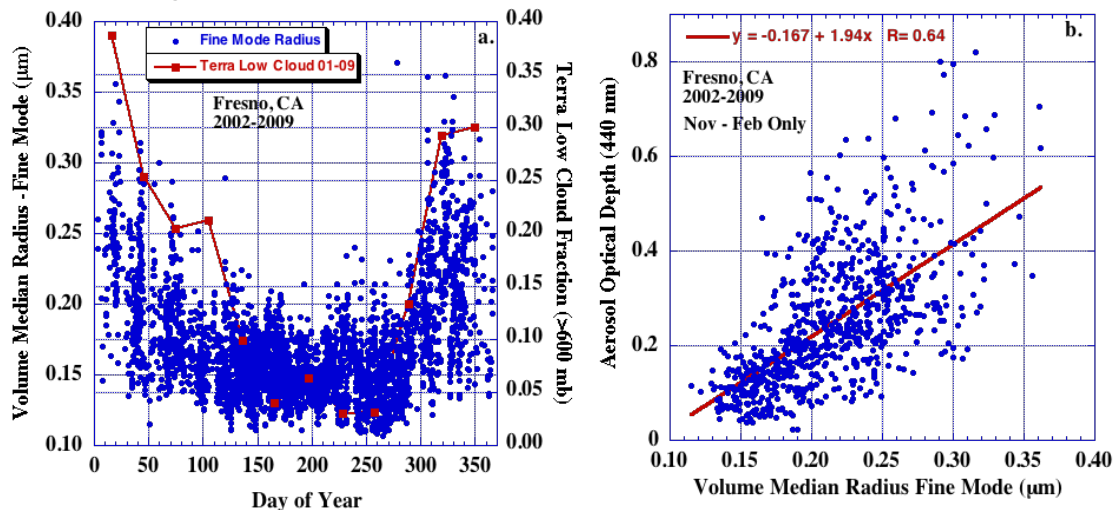


Figure 2: (a) All of the AERONET retrievals of fine mode radius made at Fresno versus day of the year for the time interval of 2002–2009. Also shown is the monthly mean low cloud fraction from Terra MODIS (cloud top >600 mb) averaged over the 2001 through 2009 interval. (b) Relationship between fine mode radius and aerosol optical depth at 440 nm at Fresno is shown for retrievals made during the months of November through February only.



Name: Tom Eck and Brent Holben, NASA GSFC, Code 618
E-mail: Thomas.F.Eck@nasa.gov
Phone: 301-614-6625

References:

Eck, T. F., et al. (2012), **Fog- and cloud-induced aerosol modification observed by the Aerosol Robotic Network (AERONET)**, *J. Geophys. Res.*, 117, D07206, doi:10.1029/2011JD016839.

Holben, B.N. et al., **AERONET - A federated instrument network and data archive for aerosol characterization**, *Remote Sensing of Environment*, 66, 1-16, 1998.

Data Sources: The measurements we have analyzed were made by sun-sky radiometers that are a part of NASA's AErosol RObotic NETwork (AERONET; Holben et al., 1998)), which is a federated global network of standardized radiometers calibrated to consistent reference sources and processed with state of the art algorithms. Over 400 sites located in diverse environments on all continents and oceanic islands are currently a part of AERONET.

The AERONET sites in Kanpur (Indo-Gangetic Plain, northern India), Arica (Chile; Pacific coast adjacent to large stratocumulus field) and Fresno (California, San Joaquin Valley) are all in regions that experience seasonal low altitude clouds or fog. Monitoring of aerosol optical properties at these sites has been accomplished for multiple years and from 6-8 years of data were analyzed at each site investigate to the interaction between fog and/or low altitude clouds and aerosols (Eck et al., 2012). In addition to in depth studies at these sites, AERONET data at other sites were also analyzed, including the GSFC site.

Technical Description of Figures:

Figure 1: Almucentar size distribution retrievals from Fresno, CA on the morning of 11 February 2006 over a time interval of 3 h for these almucentar scans. The larger of the sub-micron modes (likely cloud processed) shows a peak radius decreasing from ~ 0.50 to $\sim 0.45 \mu\text{m}$, while the smaller mode also remained relatively constant at ~ 0.22 to $\sim 0.19 \mu\text{m}$ (the slight decrease of the smaller mode may be related to decreasing RH) over the time interval of ~ 3 hrs.

Figure 2: (a) All of the individual AERONET retrievals of fine mode radius made at Fresno versus day of the year for the time interval of 2002–2009. Also shown is the monthly mean low cloud fraction from Terra MODIS (cloud top >600 mb) averaged over the 2001 through 2009 interval. The coinciding occurrence of larger fine mode radius values with higher cloud fraction of low altitude clouds from November through February is consistent with the possibility of fog/cloud processing and/or interaction. (b) Relationship between fine mode radius and aerosol optical depth at 440 nm at Fresno is shown for retrievals made during the months of November through February only. There is a significant trend of increasing AOD as fine mode radius increases ($r = 0.64$), which likely results partly from greater scattering efficiency as particle radius increases, in addition to possibly higher aerosol number concentrations being correlated with larger radius particles.

Scientific significance: Aerosol interactions with clouds are currently the largest source of uncertainty in assessment of the anthropogenic aerosol radiative forcing on climate [Intergovernmental Panel on Climate Change (IPCC), 2007]. This pertains primarily to how aerosols modify cloud properties such as albedo and lifetime, and for absorbing aerosol particles the semi-direct effect of suppression of convection. However, the related modification of aerosol properties by interaction with clouds is also of significant importance in accurately assessing aerosol evolution and direct radiative forcing. This paper presents an investigation of aerosol processing by clouds or fog, from analysis of AERONET remote sensing retrievals.

Relevance for future science and relationship to Decadal Survey: The interaction of aerosols and clouds and resultant effects on aerosol optical depth and size distribution currently contribute to significant uncertainties in radiative forcing of aerosols at the earth's surface and the top of the atmosphere. AERONET measurements of AOD and retrieval of aerosol optical and physical properties such as size distributions have and will continue to be utilized in climate forcing studies and in the validation of current and future satellite missions.



Satellite-based Evidence for Shrub and Tundra Vegetation Expansion in Northern Quebec 1986-2010

Douglass Morton, NASA GSFC, Code 618 and Jeffery Masek, NASA GSFC, Code 618

Warmer temperatures may lead to changes in high-latitude vegetation amount and composition. Landsat data can provide a continuous, detailed view of this process.

Time series Landsat data (1986-2010) were analyzed in a north-south transect through Quebec. NDVI trends showed that shrub and graminoid (herbaceous) leaf area increased dramatically during the last three decades, likely due to pronounced summer and winter warming in the area.

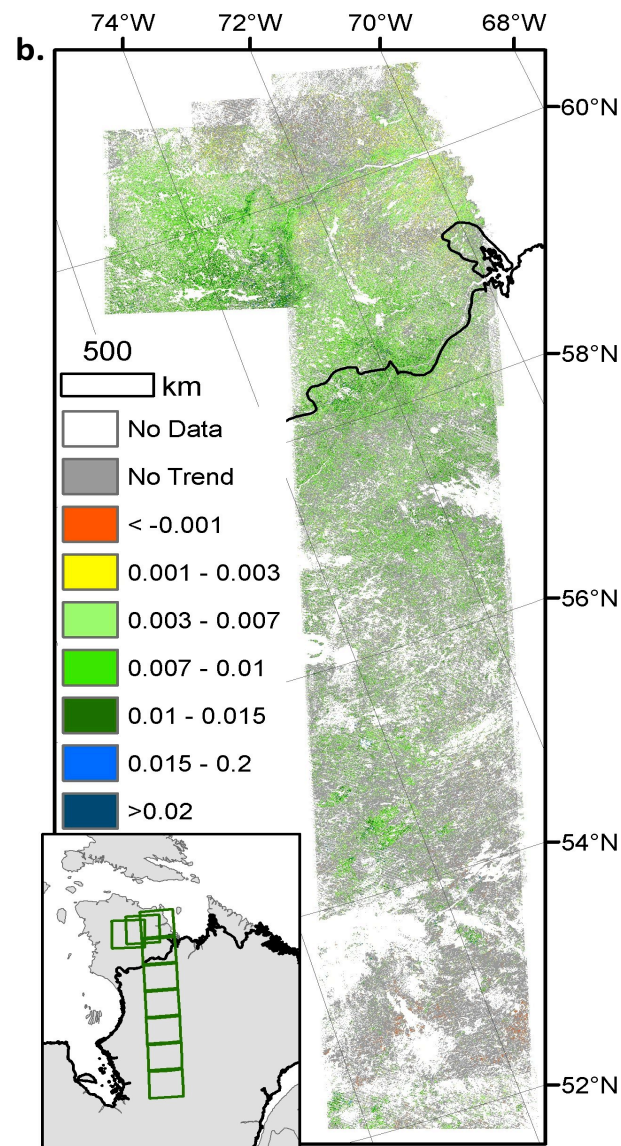


Figure 1: Landsat-based NDVI trends across northern Quebec, 1986-2010.



Name: Douglas Morton and Jeffrey Masek, NASA/GSFC, Code 618

E-mail: douglas.morton@nasa.gov

Phone: 301-614-6688

References:

McManus, K.M., D.C. Morton, J.G. Masek, D. Wang, J.O. Sexton, J. Nagol, P. Ropars, S. Boudreau (2012), Satellite-based evidence for shrub and graminoid tundra expansion in Northern Quebec from 1986-2010, in press, *Global Change Biology*

Data Sources: Long-term (1986-2010) Landsat satellite data were obtained from USGS EROS and corrected to surface reflectance and NDVI using the GSFC LEDAPS software. A total of 52 Landsat scenes spread across 9 path/row frames was used in the analysis. Comparisons with surface temperature trends (CRU TS3.1 data set), circa-2000 land cover (Canadian Forest Service Northern Land Cover of Canada dataset), and MODIS leaf-area index were also performed.

Technical Description of Image:

Figure 1: The magnitude of the normalized-difference vegetation index (NDVI) trend assessed from multi-temporal Landsat reflectance data for the Quebec transect. NDVI trends were calculated for all valid locations (no recent disturbance; sufficient non-cloudy data) using a T-test at the 95% confidence level. Significant positive (greening) trends are abundant in the northern part of the transect, dominated by shrubs and graminoid (herbaceous) cover types. Fewer positive trends are obtained in the southern (forested) part of the transect.

Scientific significance: Changes in global vegetation patterns due to climate warming represent some of the most significant potential climate impacts expected during the next century. Monitoring nascent vegetation change using consistent satellite data is thus a science priority. The results of our study indicate that low shrubs and herbaceous vegetation have responded positively to recent warming. In the tundra portion of the study area, we estimated that these greening trends corresponded to an overall increase in leaf area index (LAI) of 0.2-0.3. This LAI change represents a 20-60% relative increase in vegetation cover for these ecosystems. This study represents the first satellite-based study of changes in high-latitude fractional vegetation cover for a large (>1 Landsat frame) region at a resolution sufficient to disambiguate changes within specific land cover classes.

Relevance for future science and relationship to Decadal Survey: Future studies can expand our understanding of changes in shrub tundra by applying the Landsat-based methods in this study under a wider range of climate conditions. The upcoming LDCM mission will continue the data record necessary for tracking changes in vegetation composition and cover. The addition of space-based lidar (formerly part of the DESDynI mission) would also enable a more detailed understanding of high-latitude changes in vegetation structure (e.g. forest expansion).



Intercomparison of MODIS Albedo Retrievals and In-Situ Measurements across the Global FLUXNET Network

Alessandro Cescatti (EU-JRC), Barbara Marcolla (IASMA), Suresh K. Santhan Vannan (ORNL), Jerry Yun Pan (ORNL), Miguel O. Román (NASA/GSFC, Code 619), Xiaoyuan Yang (BU), Crystal Schaaf (UMB), et al.

Comparison of MODIS albedo retrievals with measurements taken at 53 FLUXNET sites that met strict conditions of land cover homogeneity.

A good agreement between MODIS derived mean annual values and tower-based measurements was found ($r^2 = 0.82$).

The mismatch is correlated with the spatial heterogeneity of surface albedo; stressing the relevance of spatially-representative in-situ data when validating satellite products.

Figure 2: Classification of four FLUXNET sites according to their spatial representativeness at the resolution of MODIS satellite imagery ($\sim 1 \text{ km}^2$).

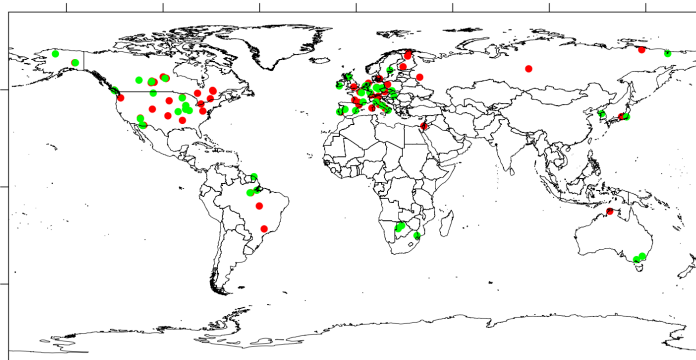


Figure 1: Spatial distribution of the 120 FLUXNET sites for which albedo measurements are available.

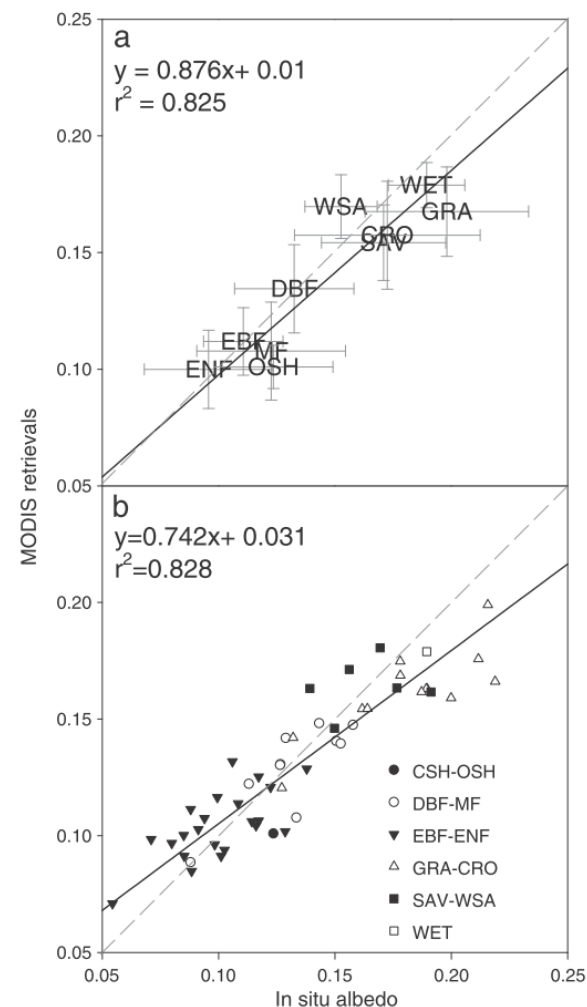
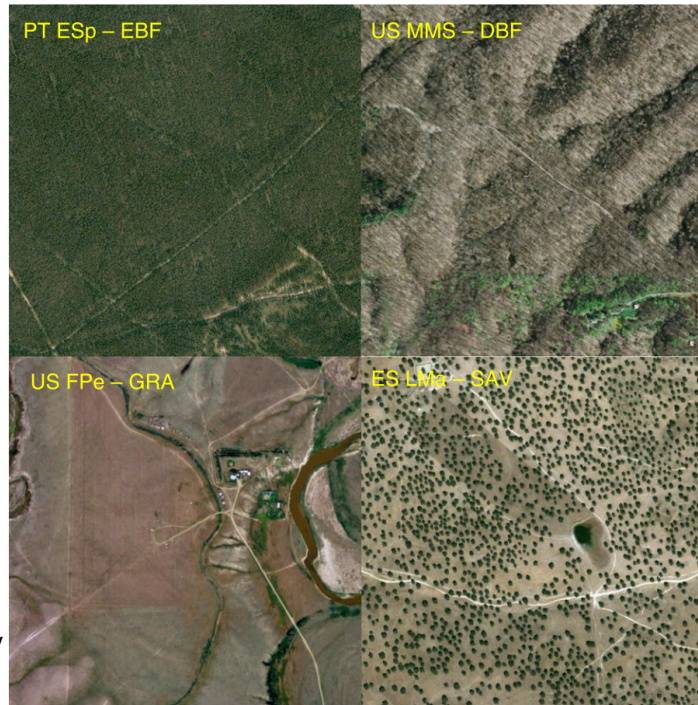


Figure 3: MODIS albedo retrievals vs. in-situ observations grouped by plant functional types (PFTs) (a), and by individual sites classified by PFT (b).



Name: Miguel O. Román, NASA/GSFC, Code 619

E-mail: Miguel.O.Roman@nasa.gov

Phone: 301-614-5498



References:

- Cescatti, A., Marcolla, B., Vannan, S.K.S., Pan, J.Y., Román, M.O., Yang, X., Ciais, P., Cook, R.B., Law, B.E., Matteucci, G., Migliavacca, M., Moors, E., Richardson, A.D., Seufert, G., & Schaaf, C.B. (2012). Intercomparison of MODIS albedo retrievals and in situ measurements across the global FLUXNET network. *Remote Sensing of Environment*, 121, 323-334. doi:10.1016/j.rse.2012.02.019.
- Román, M.O., Schaaf, C.B., Yang, X., Woodcock, C.E., Strahler, A.H., et al., (2009). The MODIS (Collection V005) BRDF/albedo product: Assessment of spatial representativeness over forested landscapes. *Remote Sensing of Environment*, 113, 2476-2498. doi:10.1016/j.rse.2009.07.009.
- Schaaf, C.B., Cihlar, J., Belward, A., Dutton, E., & Verstraete, M. (2009). *Albedo and Reflectance Anisotropy, ECV-T8: Assessment of the status of the development of standards for the Terrestrial Essential Climate Variables*. Rome: FAO.

Data Sources: This is a joint effort composed of multiple agencies including the European Commission Joint Research Centre (lead author), Oak Ridge National Laboratory's Environmental Sciences Division (processing of MODIS data), Boston University's Center for Remote Sensing (MODIS BRDF/Albedo group), and NASA-GSFC's Terrestrial Information Systems Laboratory (algorithm development and validation support). Radiometric measurements acquired by the FLUXNET community and in particular by the following networks: AmeriFlux, AfriFlux, AsiaFlux, CarboAfrica, CarboEuropeIP, CarboItaly, CarboMont, ChinaFlux, FLUXNET-Canada, Green-Grass, KoFlux, LBA, NECC, OzFlux, TCOS-Siberia, and USCCC.

Technical Description of Images:

(Figure 1) Spatial distribution of the 120 FLUXNET sites for which albedo measurements are available. Green dots correspond to sites where ground-based albedo measurements can spatially represent the satellite data at a 1 km² scale.

(Figure 2) Examples of high resolution Google Earth™ images used to visually classify the FLUXNET sites according to land cover homogeneity. Images cover an area of 1 km² centered at the tower coordinates.

(Figure 3) MODIS retrievals versus in situ observations of clear-sky and snow-free albedo. a) Averages and standard deviations of retrievals (temporal and spatial variability are accounted for) grouped by plant functional types (PFT), b) average ground measurements and retrievals at individual sites classified by PFT.

Scientific significance: Surface albedo is an essential climate variable (Schaaf et al., 2008) and accurate global estimations for all surface types during all seasons are required for climate and biogeochemical modeling efforts (Dickinson, 1995; Lofgren, 1995; Oleson, et al., 2003; Ollinger et al., 2008; Roesch et al., 2004; Tian et al., 2004). **This work has provided the mechanism for establishing the accuracy of MODIS 500m operational albedos at Stage 3 under CEOS-LPV Validation guidelines; whereby uncertainties are characterized in a statistically robust way over multiple locations and time periods representing global conditions.**

Relevance for future science and relationship to Decadal Survey: This work provides a comprehensive intercomparison of in-situ measurements and satellite retrievals of snow-free broadband surface albedo as a function of surface heterogeneity, PFT, and seasonality. The results of this investigation clearly show the need to characterize the spatial heterogeneity of reference sites using a combination of surface measurements, airborne, and fine-scale satellite imagery.